COUPLED NEOCLASSICAL-MAGNETOHYDRODYNAMIC SIMULATIONS OF AXISYMMETRIC PLASMAS

BRENDAN CARRICK LYONS

56TH ANNUAL MEETING OF THE APS DIVISION OF PLASMA PHYSICS
NEW ORLEANS, LOUISIANA
THURSDAY, OCTOBER 30, 2014

Acknowledgments

- Collaborators
  - Stephen Jardin (adviser)
  - Jesus Ramos
- Funding
  - DOE grant numbers DE-FC02-08ER54969 and DE-AC02-09CH11466
  - DOE Office of Science Graduate Fellowship Program
  - Princeton Plasma Physics Laboratory
  - Princeton University Program in Plasma Physics

Hybrid-type instabilities

- Neoclassical physics plays important role in many magnetohydrodynamic (MHD) instabilities
- Bootstrap current effects:
  - Neoclassical tearing modes (NTMs)
  - Sawtooth oscillations
  - Peeling-ballooning & edge-localized modes (ELMs)
- Neoclassical toroidal viscosity (NTV) torque impacts plasma rotation
  - Resistive wall modes
  - Locked modes
- High-fidelity simulations of these instabilities must incorporate both physical models

Framework for hybrid solver

- Use existing MHD time-evolution code (e.g., M3D-C^1, NIMROD) to evolve the Maxwellian dynamics
- New drift–kinetic equation (DKE) solver needed to solve for the non-Maxwellian dynamics
  - Self-consistency with MHD equations
  - Time-dependent
  - Full Fokker-Planck-Landau collision operator
  - Continuum model
  - Three-dimensional toroidal geometry
- Moments of DKE solution used to close MHD equations

Ramos form of DKE

- J.J. Ramos (Phys. Plasmas 2010 & 2011) provides analytic framework for a neoclassical solver appropriate for core plasma instability simulations
- DKE evolves $\bar{f}_{NMs}$, difference between full gyroaveraged distribution function and shifting Maxwellian
- Small parameters for high-temperature fusion plasmas

$$\boxed{\delta \sim \rho_i/L \ll 1} \qquad \boxed{\hat{\nu} \sim L/\lambda_{\mathrm{mfp}} \sim \delta}$$

- Important properties:
  - Maintained to collisional inverse timescale of $O\left(\delta^3 v_{the}/L\right)$
    - Conventional neoclassical banana regime for electrons
  - Velocity w referenced to each species' macroscopic flow
  - Perturbed distribution function carries no density, parallel momentum, or kinetic energy (Chapman-Enskog-like)

Overview of new code: DK4D

- Some simplifications from full Ramos formulation
  - Ion & electron DKEs to first-order in Larmor radius parameter
  - Axisymmetric geometries
  - Equal ion and electron temperature
    - No external heat sources to drive a difference
  - Pressure and temperatures are flux functions
- These assumptions will be relaxed in future work, allowing for:
  - Ion DKE to second-order in Larmor radius parameter
  - Non-axisymmetric geometries with islands
  - Separate but comparable temperatures
  - Parallel temperature and density gradients

Steady-state benchmarks

- Successful convergence and Sauter benchmark studies for DK4D have been published
  - 2014 Ph.D. thesis, Princeton University
  - Associated PoP special edition paper
- Cross-code benchmark with NEO, NCLASS, and NIMROD
  - See forthcoming Phys. Plasma by E. Held et al.

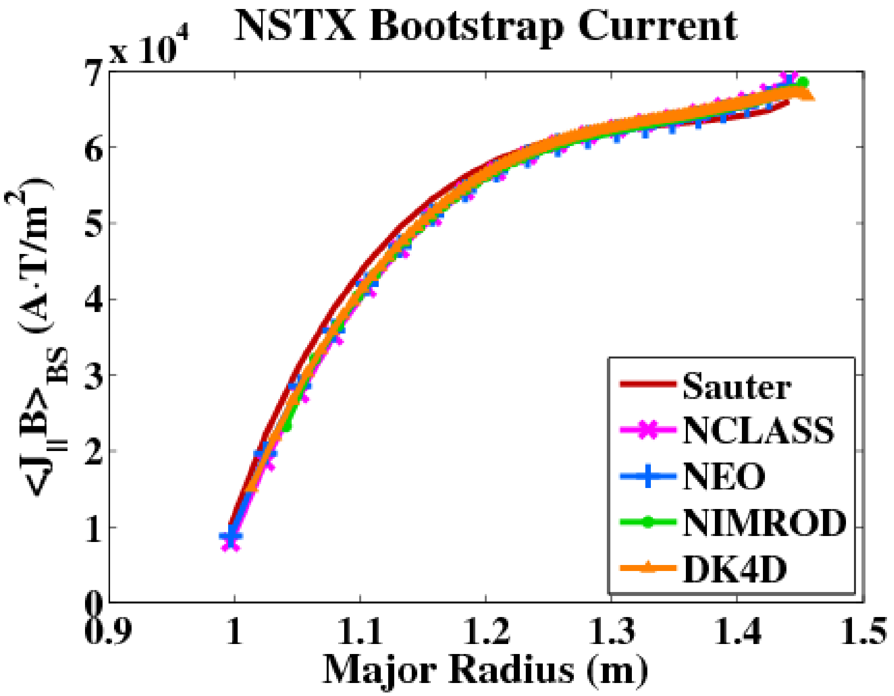

Hybrid iteration scheme

Evolve DK4D to get (possible steady-state) distribution function for given magnetic configuration

Take moments to get necessary closures for MHD equations

(e.g., friction force)

Evolve MHD equations to get new magnetic configuration using extended MHD time evolution code

1D MHD test solver

- From $\mathbf{B} = \nabla\psi \times \nabla\zeta + I\nabla\zeta$ $\quad \dfrac{\partial \mathbf{B}}{\partial t} = -\nabla \times \mathbf{E}$ $\quad \mathbf{E} + \mathbf{u} \times \mathbf{B} = \mathbf{R}$, we can show that $\boxed{\dfrac{\partial \iota}{\partial t} = -\dfrac{\partial V_L}{\partial \Phi}}$ where $\Phi = \dfrac{1}{2\pi}\displaystyle\int \mathbf{B} \cdot \nabla\zeta \, dV$, $\iota = -2\pi \dfrac{d\psi}{d\Phi}$, and $V_L = -2\pi \dfrac{\langle \mathbf{B} \cdot \mathbf{R} \rangle}{\langle \mathbf{B} \cdot \nabla\zeta \rangle}$
- Assume a large aspect ratio, expansion equilibrium, enforced at each time step
- Proportional-integral-differential (PID) current controller applies loop voltage at edge
- Rotational transform advance and Grad-Shafranov solve with finite difference methods

Ohm's laws

- Three considered
  - Resistive: $\mathbf{R}_r = \eta \mathbf{J}$
  - Steady-state neoclassical: $\mathbf{R}_{neo} = \eta \left(\mathbf{J} - \mathbf{J}_{BS} \right)$
  - Drift-kinetic (from stationary electron momentum eq.)

$$\mathbf{R}_{DK} = \frac{1}{en} \left\{ \mathbf{J} \times \mathbf{B} - \frac{d\left(nT_e\right)}{d\tilde{\Phi}} \nabla\tilde{\Phi} - \nabla \cdot \left[\left(p_{e\|} - p_{e\perp} \right) \left(\mathbf{bb} - \overset{\leftrightarrow}{\mathbf{I}} /3 \right) \right] + \mathbf{F}_e^{coll} \right\}$$

  - Pressure anisotropy and collisional friction force are moments calculated from DK4D solutions
- Only resistive can be treated fully implicitly
- For stability, we use $\mathbf{R} \Rightarrow \mathbf{R}^n + \eta_{Sptz} \left(\mathbf{J}^{n+1} - \mathbf{J}^n \right)$

Current ramp-up

- Ramp-up of toroidal current from one fixed value to another over time
- Current controller maintains value close to set point

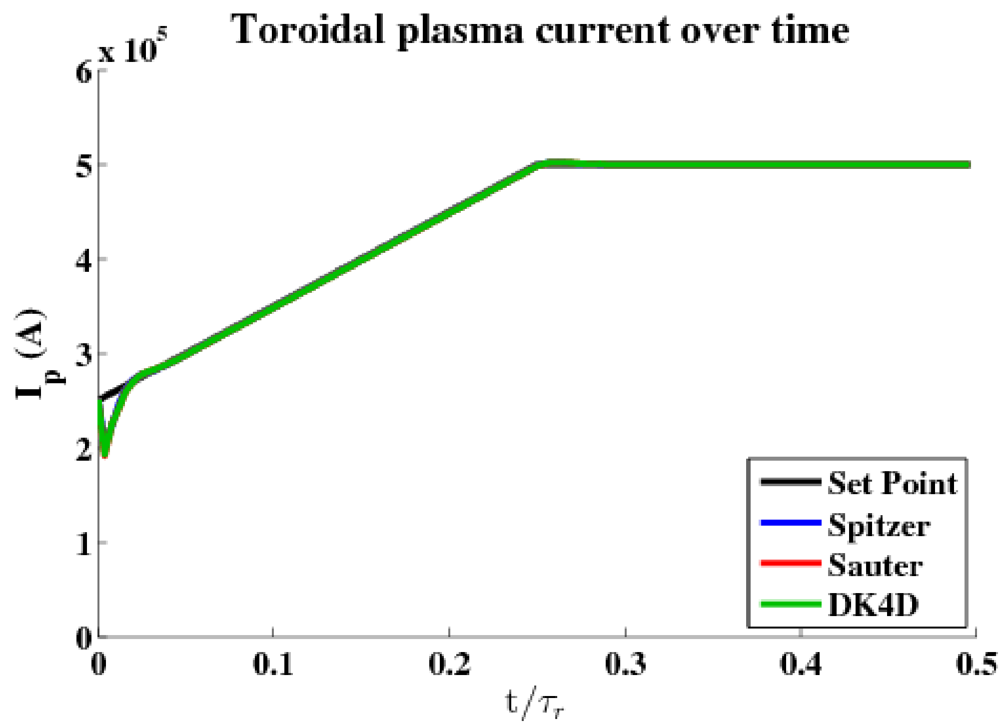

- Several density and temperature profiles considered
  - Flat, stationary density and temperatures
  - Increasing ∇n with stationary ∇T_s

No ∇n or ∇T_s - results

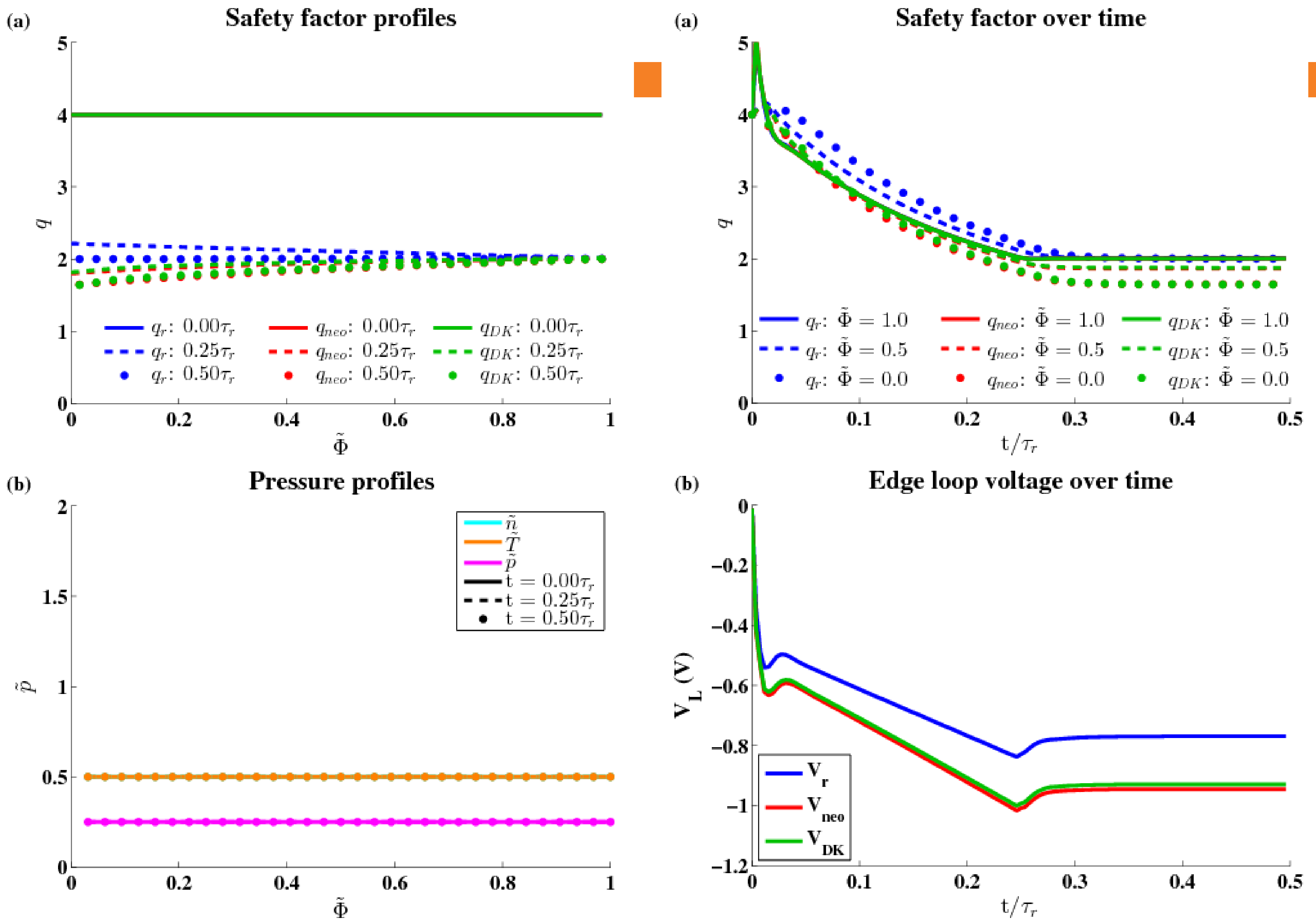

No ∇n or ∇T_s - conclusions

- Spitzer resistive case (blue)
  - Peaked safety factor as current initially driven at edge
  - Flat safety factor profile in steady-state due to uniform resistivity and no bootstrap current
  - $V_r \approx -0.77$ V
- Sauter neoclassical case (red)
  - Conductivity decreases with increasing radius
  - Hollow safety factor profile in steady-state
  - $V_{neo} \approx -0.95$ V: Larger due to higher resistivity
- DK4D drift-kinetic case (green)
  - Good agreement with Sauter in space and time
  - Due to long resistive time compared to collision time

Increasing ∇n, no ∇T_s - results

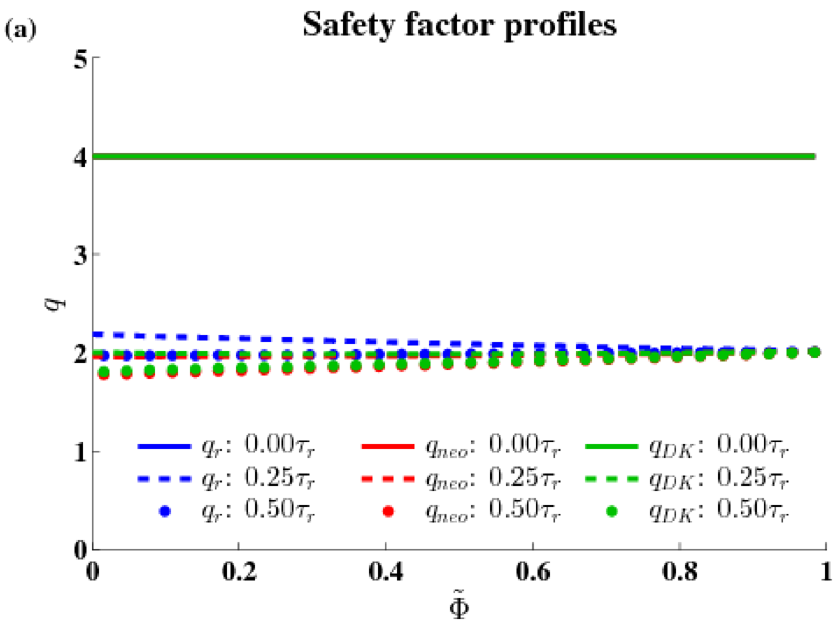

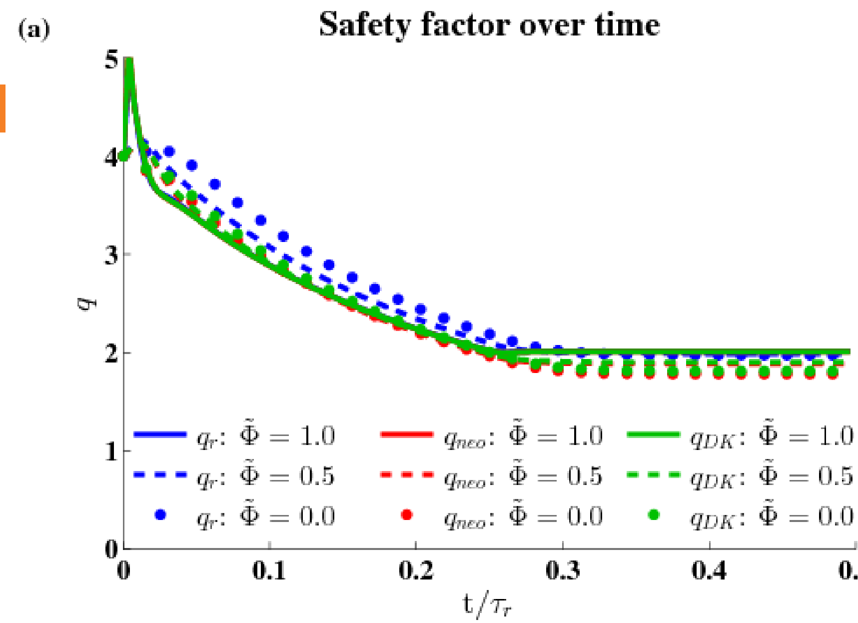

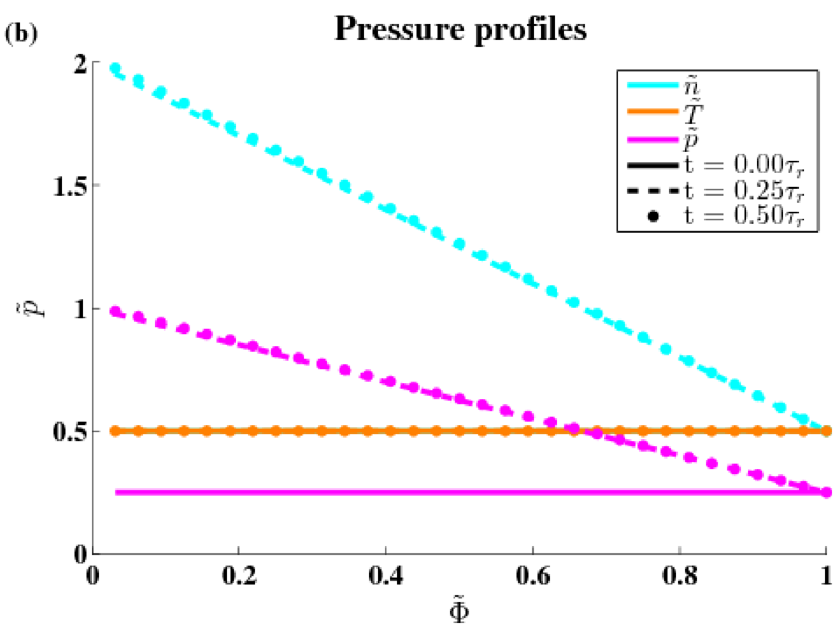

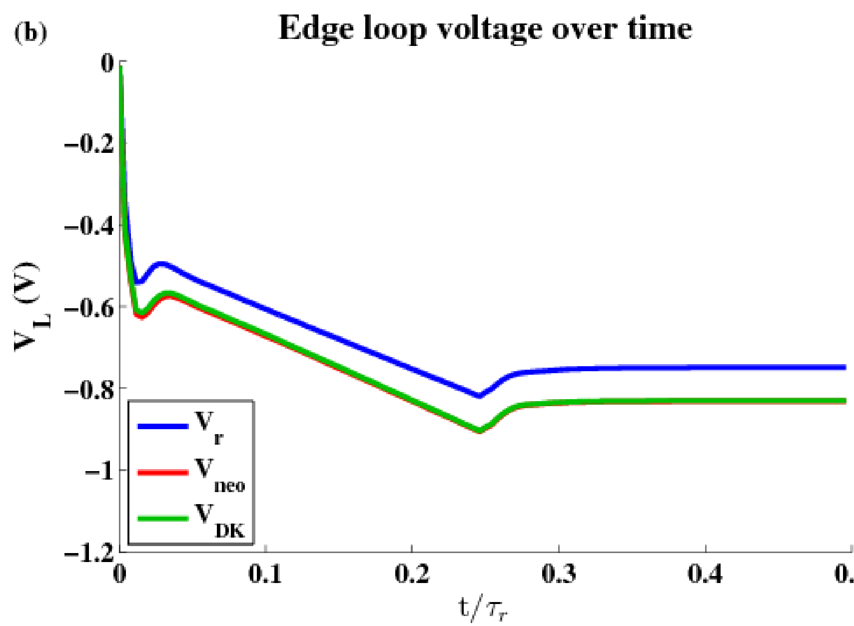

Increasing ∇n, no ∇T_s - conclusions

- Spitzer resistive case (blue)
  - Identical to previous except for slight modification in equilibrium due to pressure gradient
- Sauter neoclassical case (red)
  - Flatter profiles than previous case
    - Conductivity decreases with increasing radius
    - Bootstrap current increases with increasing radius
  - $V_{neo} \approx -0.85$ V: Smaller since there is non-inductive current
- DK4D drift-kinetic case (green)
  - Again, very good agreement with Sauter in space and time
  - No change made to Ohm's law

ELM-like pressure collapse

- Current ramp simulations showed good agreement between Sauter and DK4D since timescales were slow compared to collision time
- Preliminary work being done on quickly-evolving equilibria
- Here we examine two ELM-like pedestal pressure collapses
  - Both have same configuration in general
    - $\hat{\nu} = \tau_{transit}/\tau_{coll} = 7.64 \times 10^{-3}$
    - $\tau_{resistive}/\tau_{coll} = 2.62 \times 10^{4}$
  - Timescale of collapse differs
    - Slow collapse: $0.01\ \tau_{resistive}$ or $262\ \tau_{coll}$
    - Fast collapse: $0.001\ \tau_{resistive}$ or $26.2\ \tau_{coll}$
  - Time steps are 1/10 of pedestal collapse times
    - DK4D reaches steady-state during each “slow collapse” time step
    - Doesn’t necessarily during “fast collapse” time step

Pressure profiles

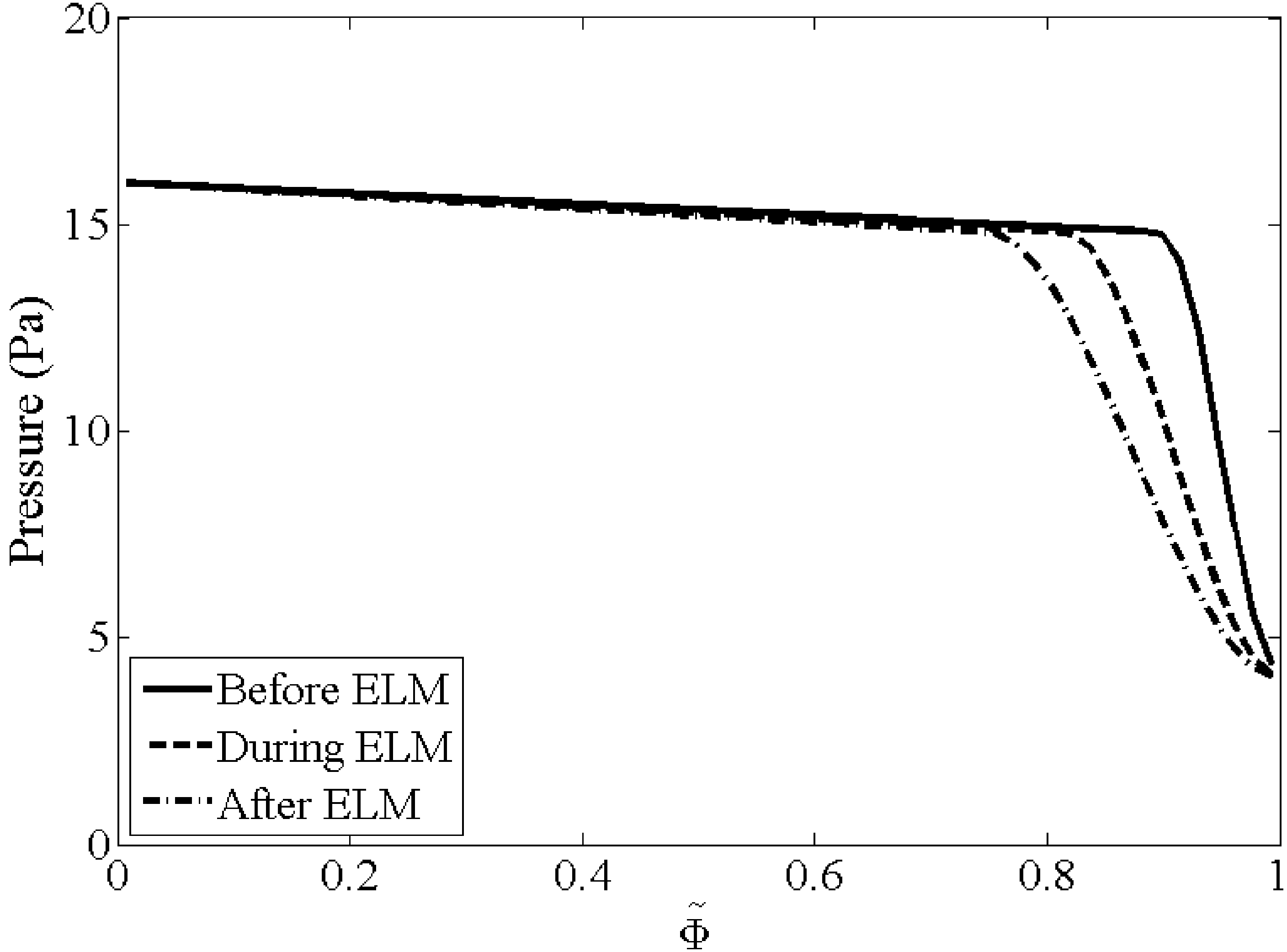

Bootstrap current over time

- Both of the "slow collapses" and Sauter's "fast collapse" all increase rapidly during ELM
- DK4D's "fast collapse"
  - Lags behind
  - Continues increasing after ELM
  - Takes time to collisionally equilibrate

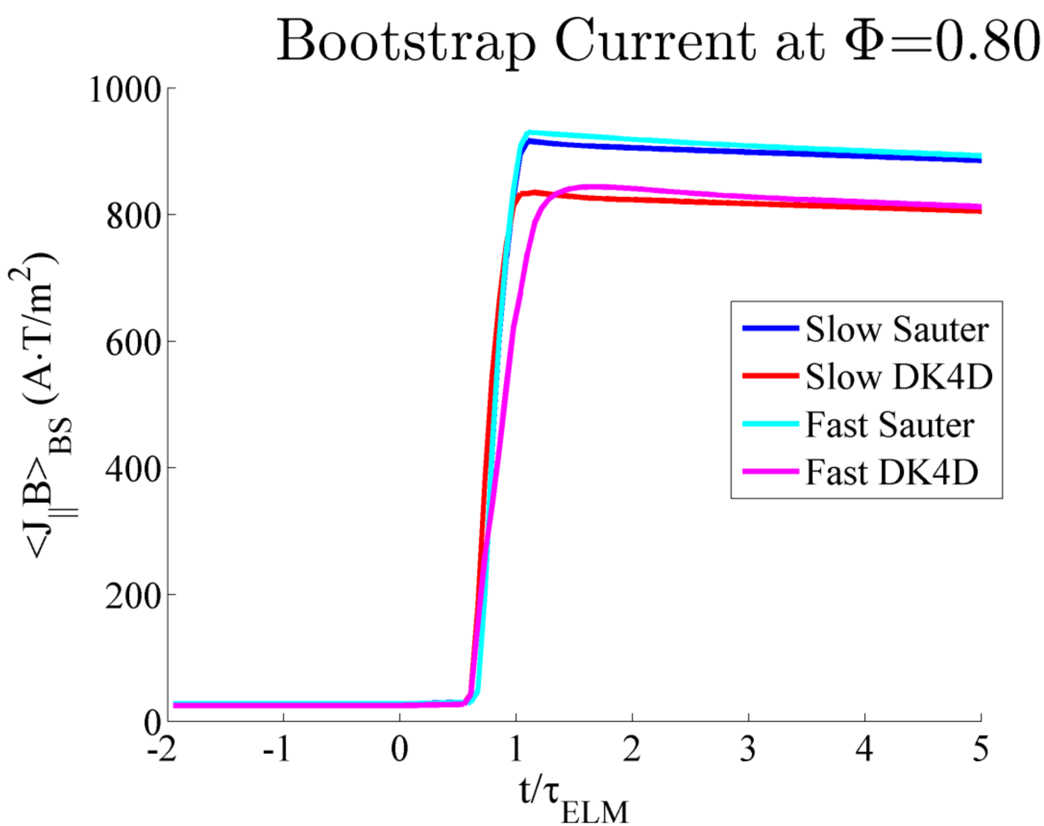

State of this work

- DK4D has some capabilities beyond other existing continuum DKE solvers
  - Time-dependent
  - Solves for distribution function
  - Solves in reference frame of macroscopic flow
  - Straight-forward, self-consistent coupling with MHD equations
- Hybrid simulations are first of their kind
  - Dynamic evolution of distribution functions and ohmic & bootstrap currents in changing magnetic equilibrium
  - In slowly-evolving equilibria, one steady-state solution is self-consistently evolved to the next, verifying use steady-state neoclassical Ohm's laws
  - In quickly-evolving equilibria, preliminary DK4D hybrid simulations demonstrate lag compared to steady-state model

Future work

- Improve and extend DK4D
  - Investigate alternate (better?) representations
    - Finite elements in y and θ to improve convergence at low collisionality
  - Non-axisymmetric geometries
- Couple to more advanced MHD code, e.g., M3D-C^1
- Perform self-consistent simulations of 3D MHD instabilities and calculations of NTV torque

21

Additional slides

Axisymmetric drift-kinetic equations

- Axisymmetric 4D phase space
  - ψ is poloidal flux per radian, θ is the poloidal angle
  - w is the total velocity in frame of macroscopic flow
  - $y = \cos\chi$ is cosine of the pitch angle
- Cross-species collisional terms dropped for ions

$$
\begin{aligned}
&\frac{\partial \bar{f}_{NMs}}{\partial t} + wy\mathbf{b}\cdot\nabla \bar{f}_{NMs} - \frac{1}{2}w\left(1-y^2\right)\mathbf{b}\cdot\nabla\ln B\frac{\partial \bar{f}_{NMs}}{\partial y} = \left\langle C_{ss} + C_{ss'}\right\rangle_\alpha \\
&+\left\{\frac{wy}{nT_s}\left[\frac{2}{3}\mathbf{b}\cdot\nabla\left(p_{s\parallel}-p_{s\perp}\right) - \left(p_{s\parallel}-p_{s\perp}\right)\mathbf{b}\cdot\nabla\ln B - \mathbf{b}\cdot\mathbf{F}_s^{coll}\right]\right. \\
&+P_2(y)\frac{w^2}{3v_{ths}^2}\left(\nabla\cdot\mathbf{u}_s - 3\mathbf{b}\cdot\left[\mathbf{b}\cdot\nabla\mathbf{u}_s\right]\right) + \frac{1}{3nT_s}\left(\frac{w^2}{v_{ths}^2}-3\right)\nabla\cdot\left(q_{s\parallel}\mathbf{b}\right) \\
&\left.-\frac{\varsigma\left(e_s\right)I}{3m_s\Omega_s}\left[\frac{1}{2}P_2(y)\frac{w^2}{v_{ths}^2}\left(\frac{w^2}{v_{ths}^2}-5\right) + \frac{w^4}{v_{ths}^4} - 10\frac{w^2}{v_{ths}^2} + 15\right]\mathbf{b}\cdot\nabla\ln B\frac{dT_s}{d\psi}\right\} f_{Ms}
\end{aligned}
$$

Collision operator

- Linearized Fokker-Planck-Landau form

$$
\begin{aligned}
\langle C_{ss} + C_{ss'} \rangle_\alpha =& \nu_{Ds}(w)\mathcal{L}[\bar{f}_{NMs}] - \nu_s f_{Ms} \frac{v_{ths}}{v_{ths'}^2} \frac{\mathbf{b}\cdot\mathbf{J}}{e_s n} \xi_{s'} y \\
&+ \frac{\nu_s v_{ths}^3}{w^2} \frac{\partial}{\partial w} \left\{ \xi_s \left[w \frac{\partial \bar{f}_{NMs}}{\partial w} + \frac{w^2}{v_{ths}^2} \bar{f}_{NMs} \right] + \xi_{s'} \left[w \frac{\partial \bar{f}_{NMs}}{\partial w} + \frac{m_s w^2}{m_{s'} v_{ths'}^2} \bar{f}_{NMs} \right] \right\} \\
&+ \frac{\nu_s v_{ths}}{n} f_{Ms} \left(4\pi v_{ths}^2 \bar{f}_{NMs} - \Phi_s[\bar{f}_{NMs}] + \frac{w^2}{v_{ths}^2} \frac{\partial^2 \Psi_s[\bar{f}_{NMs}]}{\partial w^2} \right)
\end{aligned}
$$

- Poisson equations for the Rosenbluth potentials

$$
\frac{d}{dw}\left(w^2 \frac{\partial \Phi_s}{\partial w} \right) + \frac{\partial}{\partial y}\left[\left(1 - y^2\right) \frac{\partial \Phi_s}{\partial y} \right] = -4\pi w^2 \bar{f}_{NMs}
$$

$$
\frac{d}{dw}\left(w^2 \frac{\partial \Psi_s}{\partial w} \right) + \frac{\partial}{\partial y}\left[\left(1 - y^2\right) \frac{\partial \Psi_s}{\partial y} \right] = w^2 \Phi_s
$$

Time advancement of electron DKE

$$\frac{f_{NMe}^{n+1}}{\Delta t} - wy\frac{\psi_0}{\mathcal{J}B}\frac{\partial f_{NMe}^{n+1}}{\partial \theta} + \frac{1}{2}w\left(1-y^2\right)\frac{\psi_0}{\mathcal{J}B^2}\frac{\partial B}{\partial \theta}\frac{\partial f_{NMe}^{n+1}}{\partial y} - \left[\langle C_{ee} + C_{ei}\rangle - \nu_e f_{Me}\frac{v_{the}}{v_{thi}^2}\frac{J_\parallel}{en}\xi_i y\right]^{n+1}$$

$$= \frac{f_{NMe}^{n}}{\Delta t} - \frac{1}{3nT_e}\left(\frac{w^2}{v_{the}^2} - 3\right) f_{Me}\frac{\psi_0}{\mathcal{J}B}\frac{\partial}{\partial \theta}\left(\frac{q_{e\parallel}^n}{B}\right)$$

$$-\frac{wy}{nT_e}f_{Me}\left\{\frac{2}{3}\frac{\psi_0}{\mathcal{J}B}\frac{\partial}{\partial \theta}\left(p_{e\parallel} - p_{e\perp}\right)^n - \frac{\psi_0}{\mathcal{J}B^2}\frac{\partial B}{\partial \theta}\left(p_{e\parallel} - p_{e\perp}\right)^n + \left[F_{e\parallel}^{coll} - \frac{2m_e\nu_e}{3\sqrt{2\pi}e}J_\parallel\right]^n\right\}$$

$$+\left\{P_2(y)\frac{w^2}{3v_{the}^2}\left(\nabla\cdot\mathbf{u}_e - 3\mathbf{b}\cdot[\mathbf{b}\cdot\nabla\mathbf{u}_e]\right) + \nu_e\frac{v_{the}}{v_{thi}^2}\frac{J_\parallel}{en}\xi_i y - \frac{2}{3\sqrt{2\pi}}\nu_e\frac{w}{v_{the}^2}\frac{J_\parallel}{en}y\right\} f_{Me}$$

$$-\frac{1}{3m_e\Omega_e}f_{Me}\left[\frac{1}{2}P_2(y)\frac{w^2}{v_{the}^2}\left(\frac{w^2}{v_{the}^2} - 5\right) + \frac{w^4}{v_{the}^4} - 10\frac{w^2}{v_{the}^2} + 15\right]\frac{I\psi_0}{\mathcal{J}B^2}\frac{\partial B}{\partial \theta}\frac{dT_e}{d\psi}$$

- Implicit, homogeneous convective and collision operator terms
- Explicit, homogeneous moment terms
  - No stability constraints expected since these are integrals over the solution
  - Predictor-corrector option available
- Inhomogeneous drive terms

Expansions in DKE

- Velocity
  - Finite elements for w
    - Hermite cubics
    - Cubic B-splines
- Pitch angle
  - Legendre polynomials in $y = \cos \chi$
- Configuration Space
  - ψ is just a parameter (each flux surface treated locally)
  - Fourier modes in θ

DKE solution method

- Poisson equations for Rosenbluth potentials solved simultaneously with DKE at each time step
- Galerkin method creates a sparse, block diagonal matrix in w

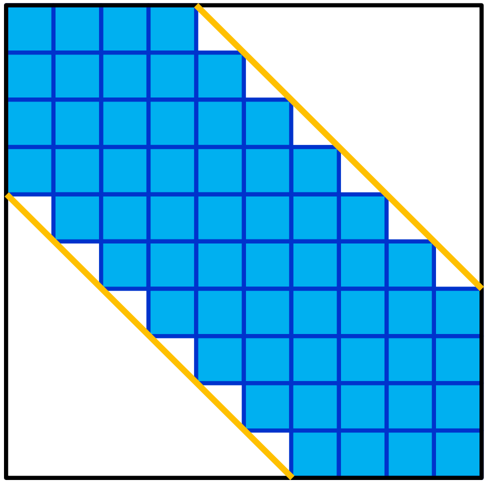

- Each block contains information on y and θ derivatives
- Two solver options implemented
  - PETSc (typically with MUMPS)
  - Sparse banded matrix using ScaLAPACK

Timescales

Device	n_G (m^{-3})	T (keV)	B (T)	I_p (MA)	a_0 (m)	R_0 (m)
LTX	3.15×10^{19}	0.2	0.34	0.067	0.26	0.40
NSTX	9.04×10^{19}	1	0.45	1.2	0.65	0.85
DIII-D	1.13×10^{20}	5	2.1	1.5	0.65	1.67
ITER	1.19×10^{20}	20	5.3	15	2.0	6.2

Device	τ_A (s)	τ_{te} (s)	τ_{ti} (s)	τ_{ce} (s)	τ_{ci} (s)	τ_r (s)
LTX	3.0×10^{-7}	6.7×10^{-8}	2.9×10^{-6}	5.8×10^{-7}	2.5×10^{-5}	3.3×10^{-1}
NSTX	8.2×10^{-7}	6.4×10^{-8}	2.7×10^{-6}	2.0×10^{-6}	8.6×10^{-5}	2.0×10^{1}
DIII-D	3.9×10^{-7}	5.6×10^{-8}	2.4×10^{-6}	1.6×10^{-5}	6.7×10^{-4}	2.0×10^{2}
ITER	5.9×10^{-7}	1.0×10^{-7}	4.5×10^{-6}	1.1×10^{-4}	4.6×10^{-3}	1.3×10^{4}

- Distribution function will likely evolve to steady state within a resistive time
- Must consider full time dependence as MHD code time steps (10-100 Alfven times) can be less than the electron collision time

Equilibria used

- From the JSOLVER equilibrium code
- Large Aspect Ratio
- NSTX

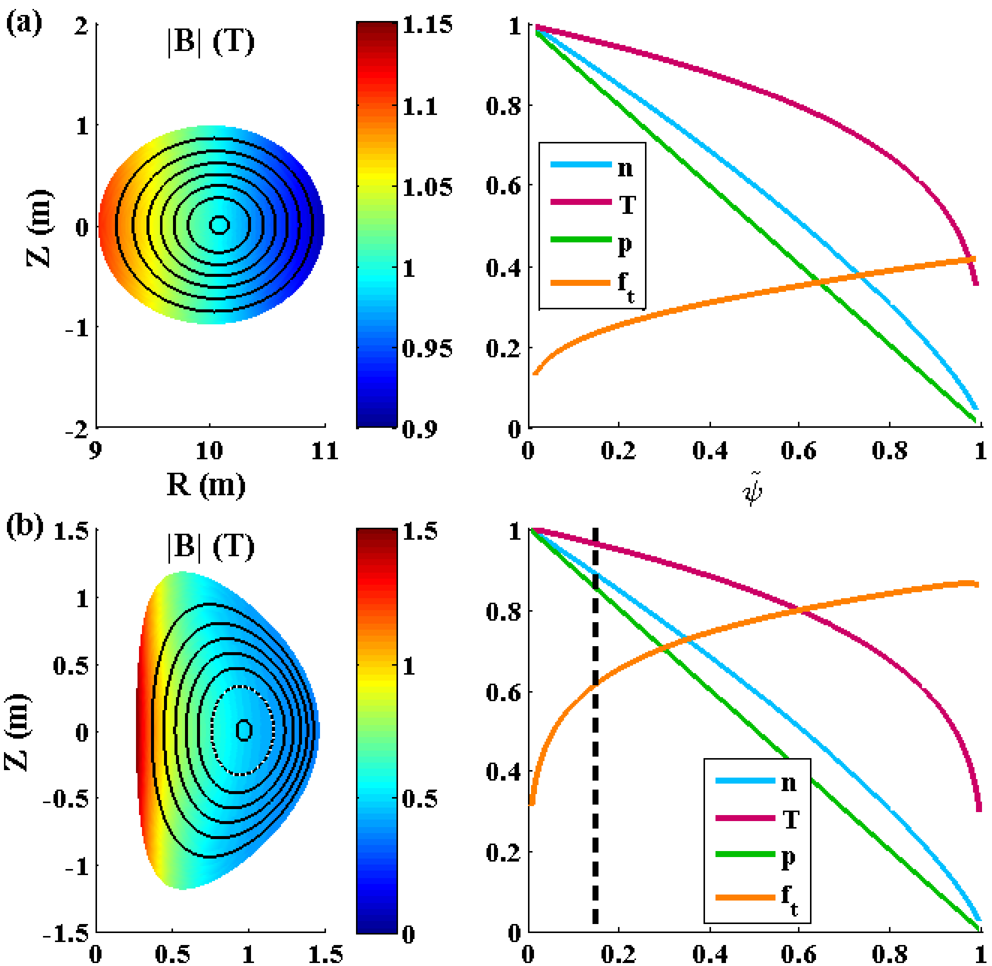

Calculating Sauter-like coefficients

- When run to steady-state, we can calculate the neoclassical conductivity and bootstrap current coefficients for an equilibrium
- Must separate inhomogeneous source terms in DKE
- Coefficients given by collisional friction force and pressure anisotropy via parallel Ohm's law

$$\langle \mathbf{J}\cdot\mathbf{B}\rangle = \sigma_{neo}\langle \mathbf{E}\cdot\mathbf{B}\rangle + I\left[\mathcal{L}_{31}\frac{dP}{d\psi} + \mathcal{L}_{32}n\frac{dT_e}{d\psi} + \alpha\mathcal{L}_{34}n\frac{dT_i}{d\psi}\right]$$

$$U_i = \alpha\frac{I}{e\langle B^2\rangle}\frac{dT_i}{d\psi}$$ where $$\mathbf{u}_i = U_i(\psi)\mathbf{B} + R^2\left[\frac{d\phi}{d\psi} + \frac{1}{en}\frac{d(nT_i)}{d\psi}\right]\nabla\zeta$$

Conductivity and L_{31} benchmark

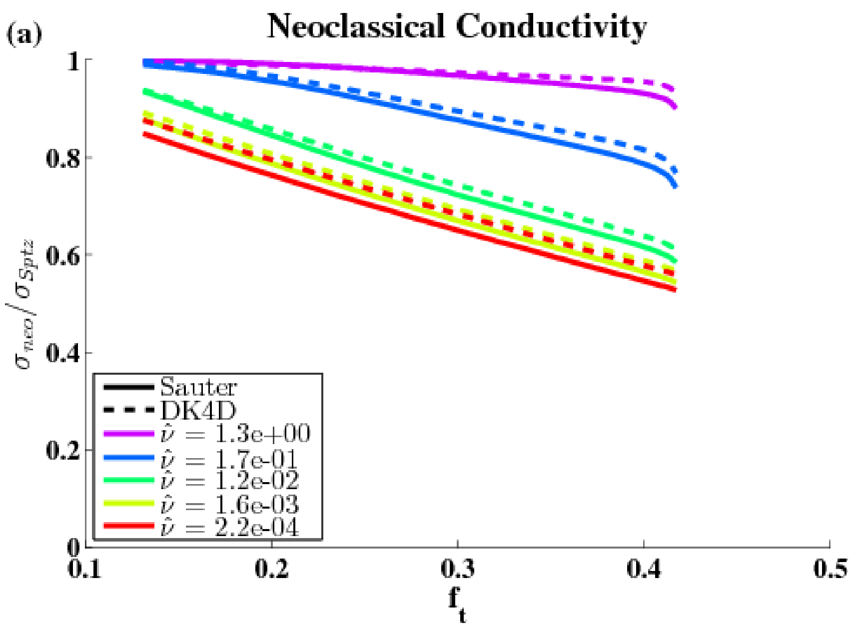

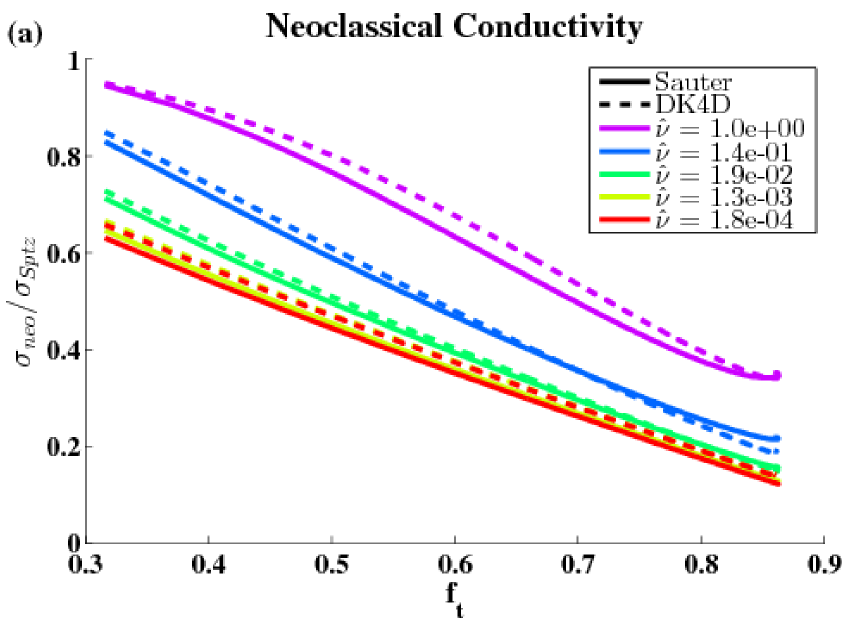

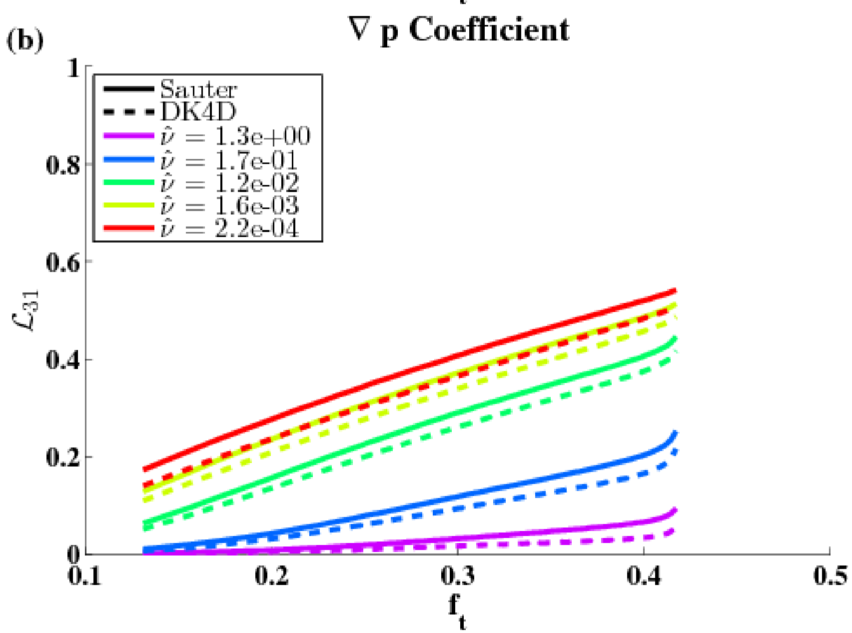

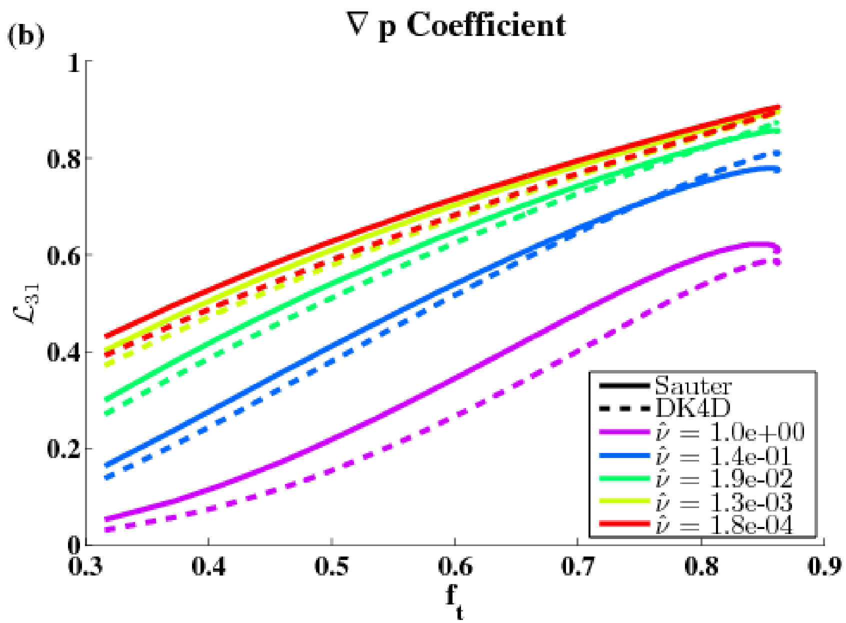

L_{32} and L_{34} benchmark

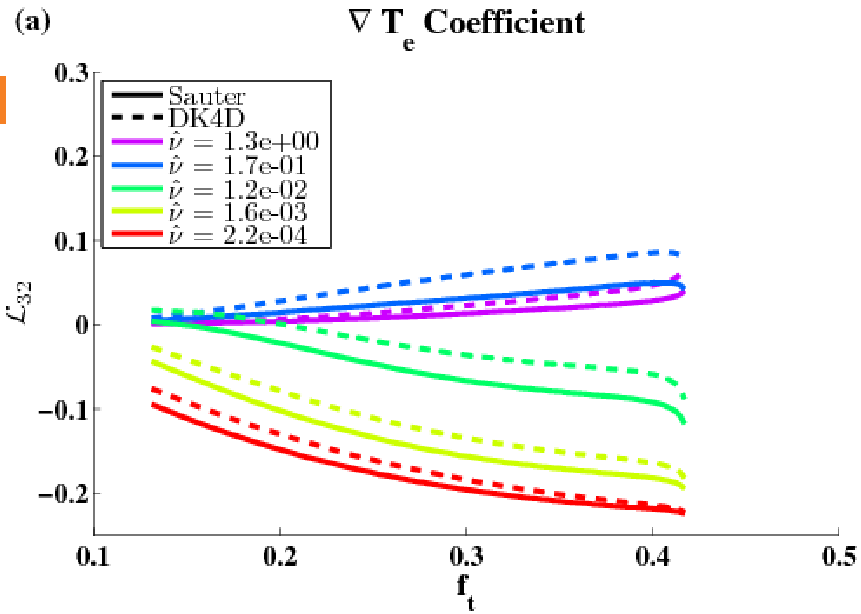

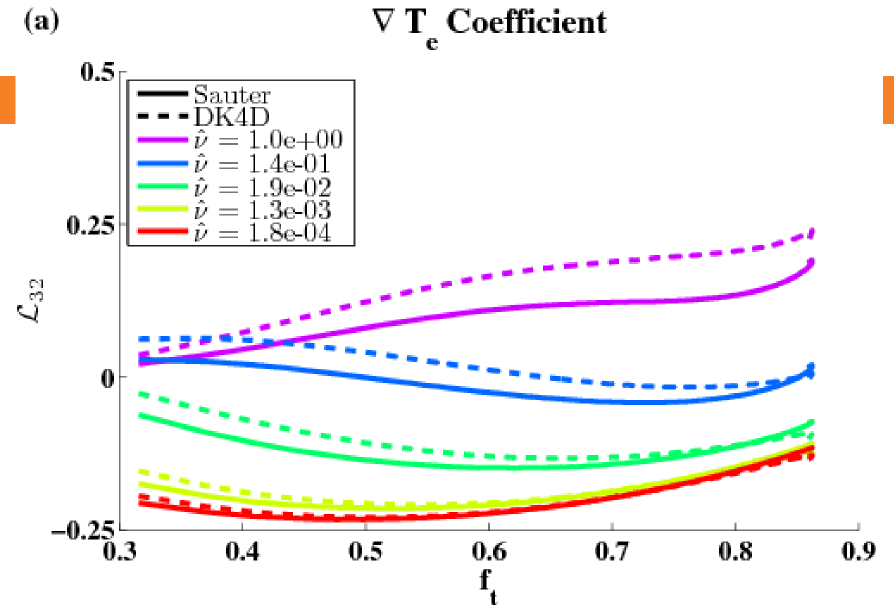

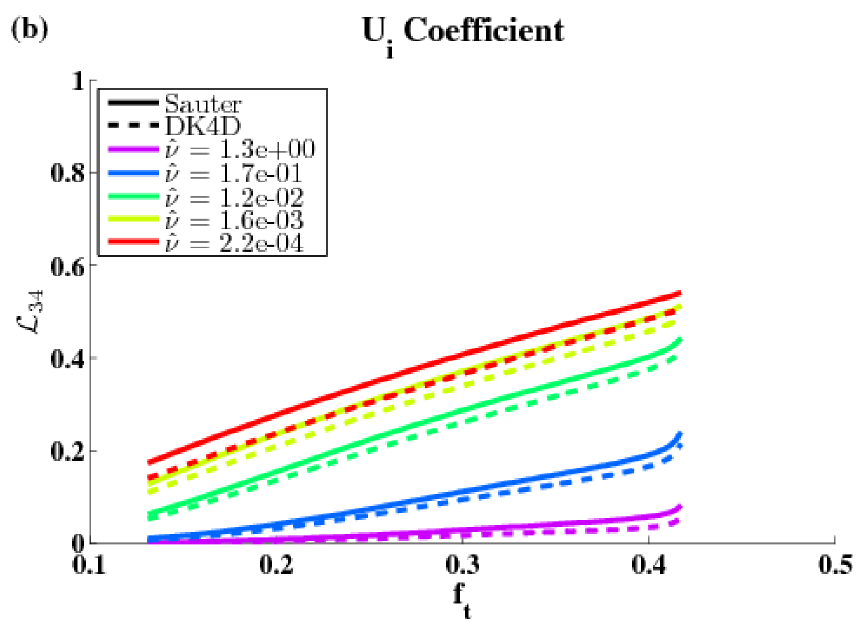

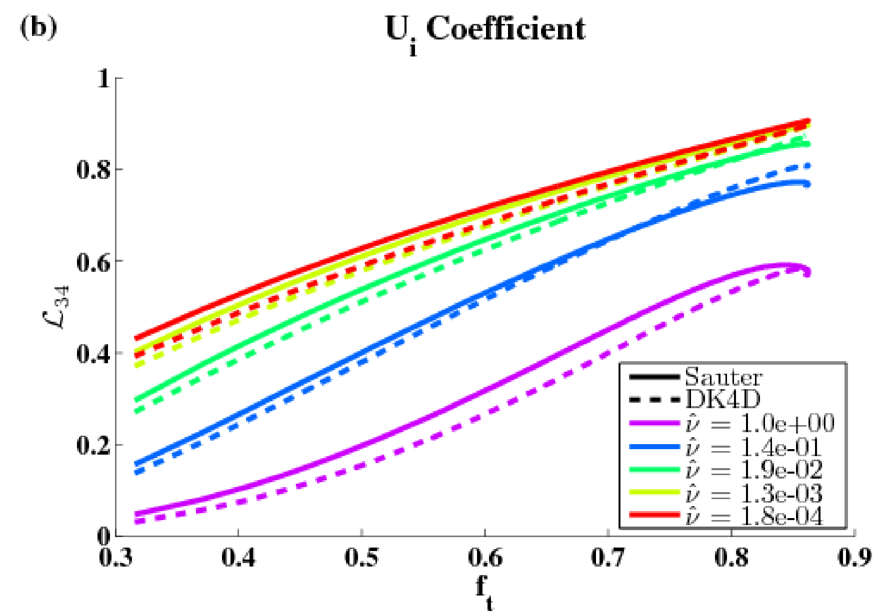

Ion flow coefficient benchmark

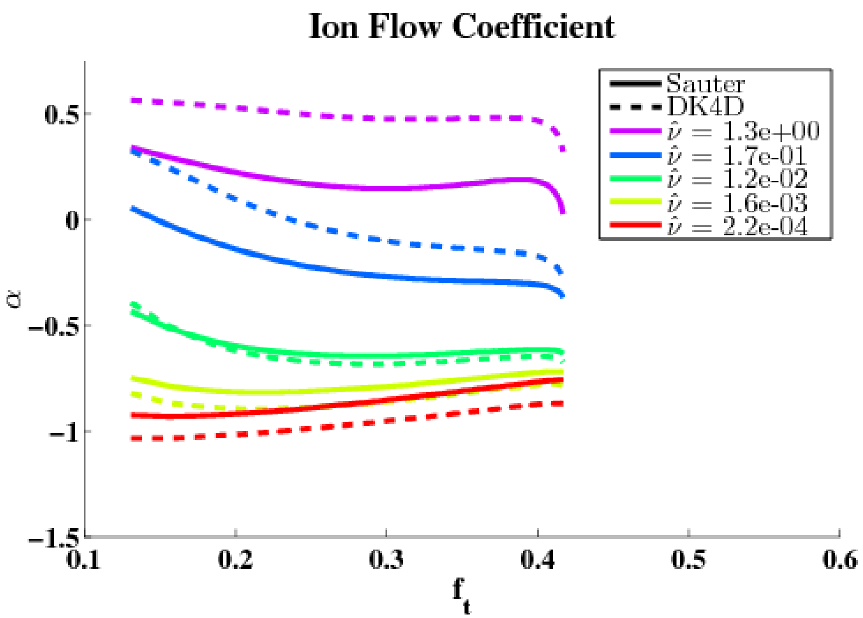

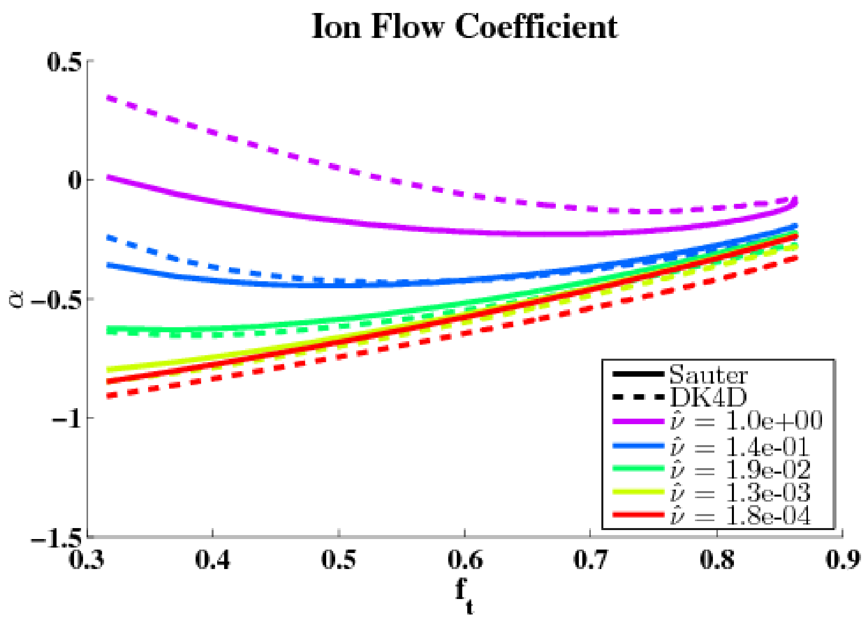

Increasing ∇n, stationary ∇T_s - results

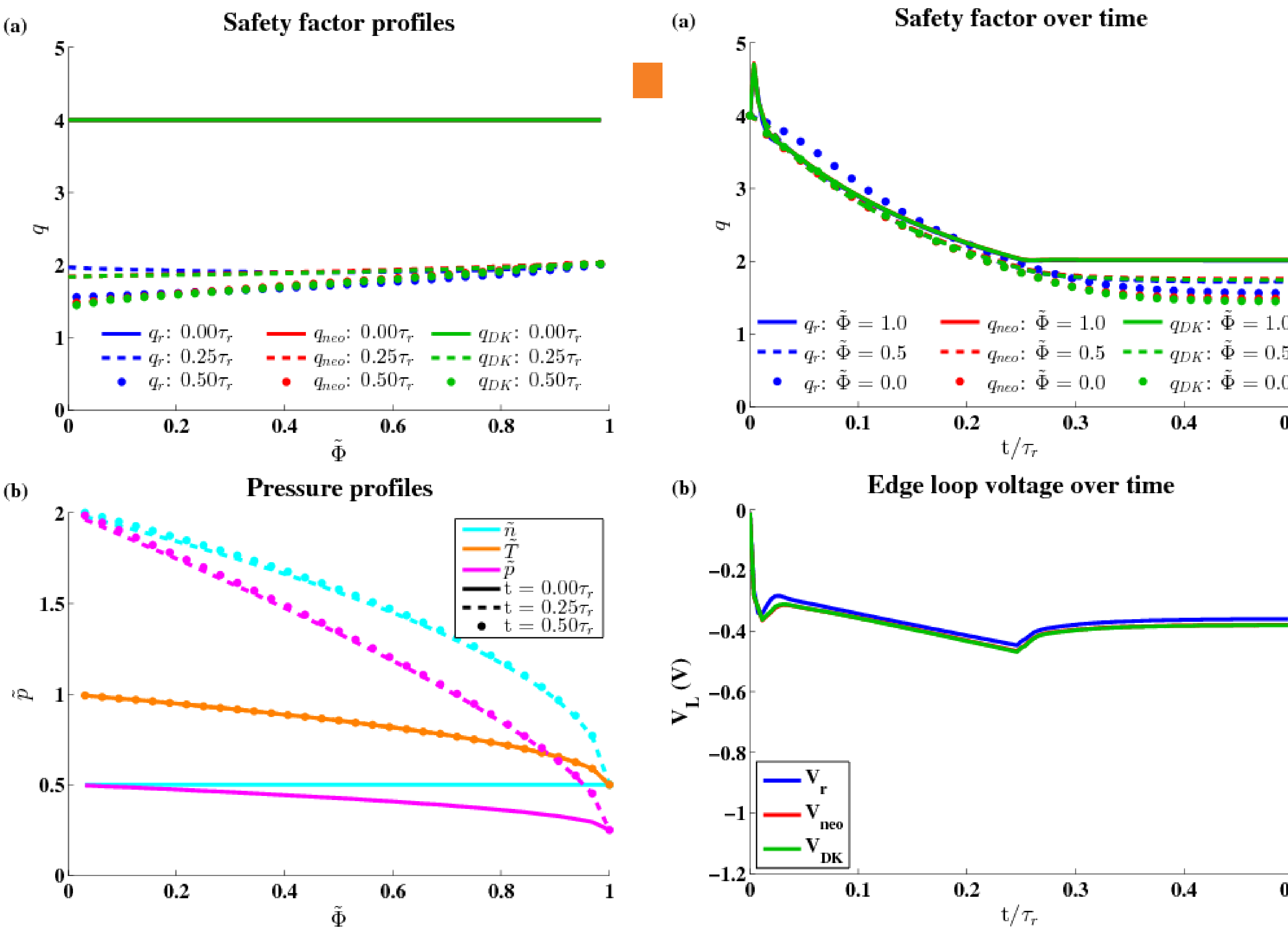

Increasing ∇n, stationary ∇T_s - concls.

- Spitzer (green) now has nonuniform resistivity
- Sauter (red) and DK4D (green) are, again, in good agreement
- Spitzer also now in good agreement
  - Coincidental near-balancing of neoclassical conductivity and bootstrap current effects
- Lower resistivity on-axis leads to more realistic hollow safety factor profiles
  - $q_{axis} \approx 1.5, q_{edge} \approx 2$
- $V_{neo} \approx -0.38$ V: Much lower due to lower resistivity